Distributed Piezoelectric-Polymer Active Vibration Control of a Cantilever Beam

Thomas Bailey* and James E. Hubbard Jr.†
Massachusetts Institute of Technology, Cambridge, Massachusetts

An active vibration damper for a cantilever beam was designed using a distributed-parameter actuator and distributed-parameter control theory. The distributed-parameter actuator was a piezoelectric polymer, poly (vinylidene fluoride). Lyapunov's second method for distributed-parameter systems was used to design a control algorithm for the damper. If the angular velocity of the tip of the beam is known, all modes of the beam can be controlled simultaneously. Preliminary testing of the damper was performed on the first mode of the cantilever beam. A linear constant-gain controller and a nonlinear constant-amplitude controller were compared. The baseline loss factor of the first mode was 0.003 for large-amplitude vibrations (±2 cm tip displacement) decreasing to 0.001 for small vibrations (±0.5 mm tip displacement). The constant-gain controller provided more than a factor of two increase in the modal damping with a feedback voltage limit of 200 V rms. With the same voltage limit, the constant-amplitude controller achieved the same damping as the constant-gain controller for large vibrations, but increased the modal loss factor by more than an order of magnitude to at least 0.040 for small vibration levels.

Introduction

SATELLITES and other large spacecraft structures are generally lightly damped due to low structural damping in the materials used and the lack of other forms of damping, such as air drag. In large structures, these vibrations have long decay times that can lead to fatigue, instability, or other problems with the operation of the structure.[1] Flexible structures are distributed-parameter systems having a theoretically infinite number of vibrational modes. Often, current design practice is to model the system with a finite number of modes and to design a control system using lumped-parameter control theory. "Truncating" the model may lead to performance tradeoffs when designing a control system for distributed-parameter systems.[2]

There exists a wealth of distributed-parameter control theory in the literature. References 3-8 are a small sampling of what is available. However, there are very few applications in the literature. One reason may be the difficulty of using distributed-parameter control theory with spatially discrete sensors and actuators. The goal of this study is to design and experimentally evaluate an active vibration damper for distributed-parameter systems using a distributed-parameter actuator and to show some advantages of distributed-parameter control theory.

A scale model of a flexible satellite has been designed and built as a test structure for active vibration control schemes.[1] (See Fig. 1.) This test structure consists of a hub mounted on an air bearing table with four perpendicular arms (1.2 m long) extending radially from the hub. The arms have either thrusters or weights for the tip mass. Accelerometers at the tip of the arms monitor the vibrations of the structure. The damper developed in this study is to be applied to the flexible arms. For the development work, an arm was modeled as a cantilever beam with a tip mass and tip inertia. A smaller dynamically scaled model of one of the arms (including the use of a tip accelerometer) was used for the preliminary testing.

Received July 1, 1984; revision received Jan. 2, 1985.

*Research Assistant.
†Assistant Professor of Mechanical Engineering. Member AIAA.

This paper presents the design and analysis of an active damper for a thin cantilever beam, describes the apparatus and procedures used in the preliminary testing of the damper, and discusses the results.

Design and Analysis

The Distributed-Parameter Actuator

The active element being used is a piezoelectric polymer, poly (vinylidene fluoride) or PVF_2. PVF_2 is a polymer that can be polarized or made piezoelectrically active with the appropriate processing during manufacture. In its nonpolarized form, PVF_2 is a common electrical insulator, among many other uses. In its polarized form, PVF_2 is essentially a tough, flexible piezoelectric crystal. Polarized PVF_2 is commercially available as a thin polymeric film. The film generally has a layer of nickel or aluminum deposited on each face to conduct a voltage or field across its faces.

A sketch of the PVF_2 is shown in Fig. 2. For uniaxially polarized PVF_2, a voltage or field applied across its faces (y direction) results in a longitudinal (x direction) strain. This is the d_{31} component of the piezoelectric activity. (Biaxially polarized PVF_2 would strain in both the x and z directions. This study uses uniaxial PVF_2.) The strain occurs over the entire area of the PVF_2 making it a distributed-parameter actuator. If the field is varied spatially, the strain will also vary spatially. This gives the added possibility of varying the control spatially as well as with time.

Modeling the Active Damper

The simplest possible damper configuration was used for this study; a layer of PVF_2 bounded to one side of the cantilever beam. A sketch of the resulting two-layer beam is shown in Fig. 3. Only transverse vibrations of the beam $w(x,t)$ will be analyzed. A subscript $(\ )_1$ refers to the original cantilever, while a subscript $(\ )_2$ refers to the PVF_2 layer.

The effect of a voltage applied to the PVF_2 is to introduce a strain, ϵ_p in the PVF_2 layer given by

$$\epsilon_p(x,t) = V(x,t) \cdot (d_{31}/h_2) \tag{1}$$

where V is the applied voltage, d_{31} the appropriate static piezoelectric constant, and h_2 the thickness (y direction) of the

PVF_2 layer. This strain has two effects on the beam. One effect is a longitudinal strain ϵ_l to insure a force equilibrium in the axial (x) direction. The steady-state value of ϵ_l is found by solving the force equilibrium and is given by

$$\epsilon_l(x) = -\frac{E_2 h_2}{E_1 h_1 + E_2 h_2} \cdot \epsilon_p(x) \tag{2}$$

where E is the modulus of elasticity and h the thickness of the layers. The other effect of the piezoelectric strain is that the net force in each layer acts through the moment arm from the midplane of the layer to the neutral axis of the beam, producing a bending moment given by

$$T(x,t) = E_1 h_1 b \epsilon_l [(h_1/2) - D]$$
$$+ E_2 h_2 b (\epsilon_p + \epsilon_l)[(h_2/2) + h_1 - D] \tag{3}$$

where b is the width of the beam (assuming that $b_1 = b_2$) and D the location of the neutral axis of the composite beam given by

$$D = \frac{E_1 h_1^2 + E_2 h_2^2 + 2 h_1 h_2 E_2}{2(E_1 h_1 + E_2 h_2)} \tag{4}$$

See Fig. 4 for a detail of the cross section of the composite beam. Combining Eqs. (1-4) and reducing yields

$$T(x,t) = -V(x,t) \cdot d_{31} \left(\frac{h_1 + h_2}{2}\right) \frac{E_1 h_1 E_2 b}{(E_1 h_1 + E_2 h_2)} \tag{5}$$
$$= V(x,t) \cdot c$$

where c is a constant (for a given beam material and geometry) expressing the bending moment per volt. If the material properties and geometry of the composite beam change along its length, then c is a function of x also.

Combining Eq. (5) with a conventional Bernoulli-Euler beam analysis yields the equations of motion for transverse vibrations $w(x,t)$ of the composite beam. The governing equation is

$$\frac{\partial^2}{\partial x^2}\left[EI\frac{\partial^2 w}{\partial x^2} - c \cdot V(x,t)\right] + \rho A \frac{\partial^2 w}{\partial t^2} = 0 \quad \text{for } 0 < x < L \tag{6}$$

with boundary conditions

$$w = \frac{\partial w}{\partial x} = 0 \quad \text{for} \quad x = 0$$

$$EI\frac{\partial^2 w}{\partial x^2} = -I_t \frac{\partial^3 w}{\partial t^2 \partial x} + c \cdot V(x,t)$$

$$EI\frac{\partial^3 w}{\partial x^3} = M_t \frac{\partial^2 w}{\partial t^2} + c \cdot \frac{\partial V(x,t)}{\partial x} \quad \text{for } x = L \tag{7}$$

where $EI = E_1 I_1 + E_2 I_2$, I is the area moment of inertia of the layer about the z axis, $\rho A = \rho_1 A_1 + \rho_2 A_2$, ρ is the density of the layer, A the cross-sectional area of the layer, and M_t and I_t the tip mass and tip inertia, respectively.

For the development work, the simplest damper would have uniform geometry and a spatially uniform voltage applied along its length. Making this assumption, the spatial derivatives for the input voltage of the system described by Eqs. (6) and (7) are zero leaving

$$EI\frac{\partial^4 w}{\partial x^4} + \rho A \frac{\partial^2 w}{\partial t^2} = 0 \qquad \text{for } 0 < x < L \tag{8}$$

with boundary conditions

$$w = \frac{\partial w}{\partial x} = 0 \qquad \text{for } x = 0$$

$$EI\frac{\partial^2 w}{\partial x^2} = -I_t \frac{\partial^3 w}{\partial t^2 \partial x} + c \cdot V(t)$$

$$EI\frac{\partial^3 w}{\partial x^3} = M_t \frac{\partial^2 w}{\partial t^2} \qquad \text{for } x = L \tag{9}$$

Notice that the control voltage appears in only one of the boundary conditions. Equations (8) and (9) describe a linear distributed-parameter system that has only boundary control. Since the actuator is spatially distributed, it was easily included in the equations of motion without nonlinear terms (e.g., spatial delta functions). This allows one to keep a linear distributed-parameter model throughout the analysis, avoiding any problems that may be caused by "truncating" the model.

Deriving a Distributed-Parameter Control Algorithm

Distributed-parameter control theory was used to design a control algorithm for the active damper. This allows one the possibility of controlling all the modes of vibration at once, provided that the system is controllable through the actuator. Hence, one may avoid problems with spillover of the uncontrolled modes.[2]

The control problem is to damp the vibrations of the system described by Eqs. (8) and (9) using the input voltage $V(t)$ to the PVF_2 as the control variable. We shall assume that there is some practical limit on the magnitude of $V(t)$, i.e., $|V(t)| \leq V_{\max}$. For the moment, assume there is no restriction on the type of sensors available.

Lyapunov's second or direct method can be used to design control algorithms and can easily deal with bounded inputs and distributed-parameter systems.[4,9] This design method was chosen because it was the most straightforward way to derive an implementable distributed-parameter control law. With this method, one finds a Lyapunov functional of the system and chooses the control to minimize the time rate of change of the functional at every point in time. An appropriate functional for the system described by Eqs. (8) and (9) is the sum of the squares of the curvature and velocity, integrated along the

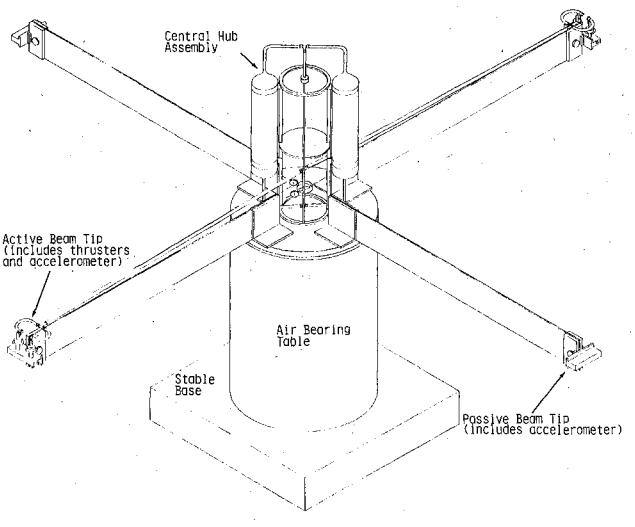

Fig. 1 Flexible test structure.

length of the beam,[10] or

$$F=\frac{1}{2}\int_0^L\left[\left(\frac{\partial^2 w}{\partial x^2}\right)^2+\left(\frac{\partial w}{\partial t}\right)^2\right]dx \tag{10}$$

This functional can be thought of as a measure of "how far" the beam is from its equilibrium position or as a measure of the energy in the system. Minimizing the time derivative of this functional is then equivalent to trying to bring the system to equilibrium as fast as possible or removing as much energy as possible from the system at each point in time. Taking the time derivative of the functional yields

$$\frac{\partial F}{\partial t}=\int_0^L\left(\frac{\partial^2 w}{\partial x^2}\cdot\frac{\partial^3 w}{\partial x^2\partial t}+\frac{\partial w}{\partial t}\cdot\frac{\partial^2 w}{\partial t^2}\right)dx \tag{11}$$

Substituting from the governing equation (8) gives

$$\frac{\partial F}{\partial t}=\int_0^L\left(\frac{\partial^2 w}{\partial x^2}\cdot\frac{\partial^3 w}{\partial x^2\partial t}-\frac{EI}{\rho A}\cdot\frac{\partial^4 w}{\partial x^4}\cdot\frac{\partial w}{\partial t}\right)dx \tag{12}$$

Integrating the second term by parts twice to introduce the boundary conditions yields

$$\frac{\partial F}{\partial t}=\int_0^L\left(1-\frac{EI}{\rho A}\right)\cdot\frac{\partial^3 w}{\partial t\partial x^2}\cdot\frac{\partial^2 w}{\partial x^2}dx - \frac{M_t}{\rho A}\cdot\frac{\partial^2 w}{\partial t^2}\cdot\frac{\partial w}{\partial t}\bigg|_L-\frac{I_t}{\rho A}\cdot\frac{\partial^3 w}{\partial t^2\partial x}\cdot\frac{\partial^2 w}{\partial tx}\bigg|_L + \frac{c\cdot V(t)}{\rho A}\cdot\frac{\partial^2 w}{\partial t\partial x}\bigg|_L \tag{13}$$

The input voltage $V(t)$ appears in only one term. Therefore, to minimize $\partial F/\partial t$, the feedback voltage should be chosen so that the term it appears in is always as negative as possible, or

$$V=-\operatorname{sgn}\left(c\cdot\frac{\partial^2 w}{\partial t\partial x}\bigg|_L\right)\cdot V_{\max} \tag{14}$$

where $\partial^2 w/\partial t\partial x\,|_L$ is the angular velocity at the tip of the beam. This means that the control voltage should be chosen with as large a magnitude as possible and should generate a bending moment $(c\cdot V)$ that opposes the angular motion of the tip of the beam. The constant c is needed as an argument of the sgn( ) function to insure the bending moment opposes the angular velocity of the tip.

This control law has several desirable characteristics. First, no modes have been truncated. This control law will (theoretically) work with any and all modes of vibration of a cantilever, since every mode has some angular motion at the tip of the beam. Second, the control law depends only on the angular velocity at the tip of the beam, not an integral along its length. This means that only one spatially discrete sensor is needed to implement this distributed-parameter control law.

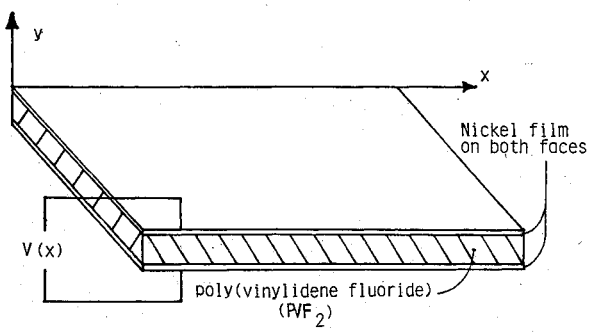

Fig. 2 Coordinate system for the PVF_2 film.

There are also several disadvantages with this control law. The sgn( ) function is nonlinear and discontinuous when its argument is zero. The discontinuous nature of this control law could lead to problems such as sliding modes and raises the difficult question of existence of solutions.[4] These problems can be avoided by replacing the sgn( ) function by a continuous one that is an arbitrarily good approximation, e.g., a saturation. A practical drawback is that the angular velocity of the tip is not readily avaiable. However, the accelerometer at the tip of the beam measures the linear acceleration that can be integrated to find the linear velocity of the tip. For any given mode of vibration, the linear velocity is directly proportional to the angular velocity, although this relation does not hold if more than one mode of vibration is present. To take advantage of this relation, it was decided to perform the preliminary testing of the damper on only one mode of vibration. The first mode was chosen because it was the easiest to isolate.

Two other control algorithms were compared against the Lyapunov control law in the preliminary testing of the damper. Written in terms of the linear velocity at the tip of beam, the three are

1) Lyapunov,

$$V(t)=-\operatorname{sgn}\left(f\cdot c\cdot\frac{\partial w}{\partial t}\bigg|_L\right)\cdot V_{\max}$$

2) Constant-gain negative velocity feedback,

$$V(t)=-k\left(f\cdot c\cdot\frac{\partial w}{\partial t}\bigg|_L\right),\quad |V(t)|\le V_{\max}$$

3) Constant-amplitude negative velocity feedback,

$$V(t)=-k(t)\left(f\cdot c\cdot\frac{\partial w}{\partial t}\bigg|_L\right),\quad |V(t)|\le V_{\max}$$

where k is a feedback gain and f a constant relating the linear velocity to the angular velocity at the tip of the beam. The constant f must be included to insure the correct phase between the linear velocity at the tip of the beam and the applied bending moment. As mentioned previously, the Lyapunov controller is nonlinear and discontinuous. The constant-gain controller can be derived from physical insight (negative velocity feedback tends to stabilize the system) or more rigorously from a modal control viewpoint. The constant-gain

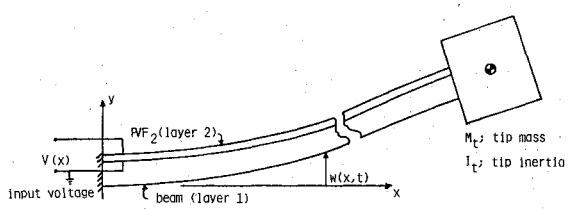

Fig. 3 Active damper configuration.

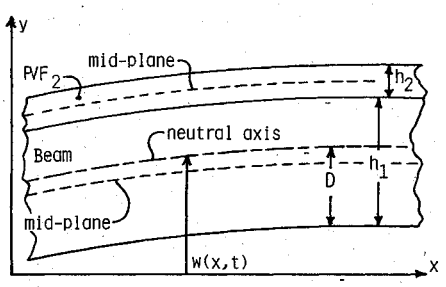

Fig. 4 Detailed cross section of beam with PVF_2 layer.

controller is linear and continuous, but as the velocity amplitude decays, so does the feedback voltage amplitude. This will reduce the effectiveness of the damper at low vibration levels for a given voltage limit. The constant-amplitude controller compensates for the decaying velocity amplitude by adjusting the feedback gain $k(t)$ to keep the amplitude of the feedback voltage constant. This controller is continuous but nonlinear and will be less effective (approximately 20%) than the Lyapunov controller, since a square wave has more area than a sine wave if they have equal amplitude. However, the constant-amplitude controller may be more practical since the control circuitry does not have to produce high-voltage step changes.

Apparatus and Procedures

The dimensions and physical properties for an arm of the test structure and for the scaled model are given in Table 1. The scale model was used for the preliminary testing. A sketch of the beam and clamping fixture is shown in Fig. 5. Included as part of the tip mass was 2 g accelerometer to monitor the vibrations of the tip of the beam. The leads to the accelerometer were made from a pair of small wires shielded inside a layer of aluminum foil and were extended above the beam from the clamping fixture to the accelerometer at the tip. This configuration provided the best shielding and had the least effect on the vibrations of the beam.

The PVF_2 film used was uniaxially polarized. Table 2 gives the dimensions and typical physical properties of the film. The PVF_2 was bonded to the steel beam using Eccobond 45LV, a low-viscosity two-part epoxy. The average adhesive thickness was 10 μm. The leads to the PVF_2 consisted of wires soldered to tabs of copper foil. The copper tabs are clamped against the nickel plating on the appropriate face of the PVF_2.

Impact testing was used to identify the natural frequencies and modal damping of the uncontrolled beam. A schematic of the equipment used in this test is shown in Fig. 6. The Hewlett-Packard 5423A spectrum analyzer applies a curve fit to the experimental data points near a resonance and uses the half-power bandwidth method to determine the modal damping. For the low levels of vibration used in impact testing, the loss factor η for the first mode was $\eta = 0.001$.

A schematic of the equipment used to implement the constant-gain and constant-amplitude controllers is shown in Fig. 7. (A controller to implement the Lyapunov control law is currently being assembled.) The accelerometer signal is integrated to give the tip velocity, phase-shifted, amplified through an audio amplifier and a step-up transformer, and applied to the PVF_2. The phase shift is necessary because the first mode of the cantilever beam is near 6 Hz, much below the linear region of an audio amplifier. The logarithmic plotter was used to determine the damping via the log decrement method. The plotter allowed a determination of how the damping changed with amplitude of vibration, especially with the nonlinear feedback of the constant-amplitude controller.

The test procedure was to hold the tip of the beam at 2 cm displacement, release it, and observe the vibrations. By holding the tip of the beam and then releasing it, very little of the second and higher modes were introduced in the initial conditions. For the constant-gain controller, the gain was set so that the maximum voltage amplitude would not exceed the voltage limit V_{max}. The maximum gain allowed was easily determined experimentally since the maximum voltage occurred when the beam was first released. For the constant-amplitude controller, the initial gain was determined in the same manner, but the gain was increased after the beam was released to keep the amplitude of the feedback voltage constant. This was done by adjusting the gain on the audio

Table 1 Beam properties

	Test structure	Scaled model
Material	Aluminum	Steel
Modulus E, $N \cdot m^{-2}$	76×10^9	210×10^9
Length L, m	1.22	0.146
Thickness h, mm	3.18	0.381
Width b, cm	15.2	1.27
Tip mass M_t, kg	2.04	6.73×10^{-3}
Tip inertia I_t, kgm^2	1.1×10^{-2}	5.0×10^{-7}
Density ρ, kgm^{-3}	2840	7800

Table 2 PVF_2 properties

Modulus E	2.0×10^9 $N \cdot m^{-2}$
Static piezoelectric constant d_{31}	22×10^{-12} mV^{-1}
Length L	0.146 m
Thickness h	28×10^{-3} mm
Width b	1.27 cm
Density ρ	1800 kg^{-3}
Breakdown voltage	1400+V

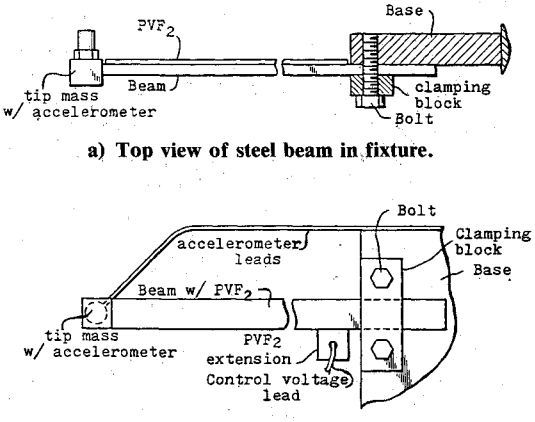

a) Top view of steel beam in fixture.

b) Side view of steel beam in fixture.

Fig. 5 Experimental beam and fixture.

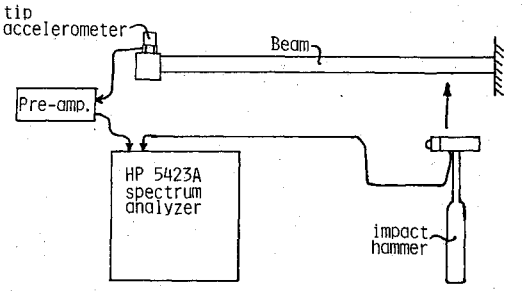

Fig. 6 Apparatus used for impact testing.

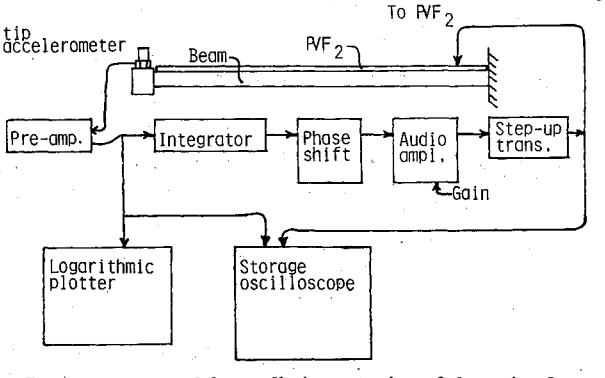

Fig. 7 Apparatus used for preliminary testing of the active damper.

amplifier while observing the feedback voltage on the oscilloscope. The gain was increased until the gain limit of the amplifier was reached.

Two voltage limits were chosen—100 and 200 V rms. These limits were dictated by safety and control circuitry limitations, not by the breakdown voltage of the PVF_2. Note in Table 2 that the breakdown voltage of the film is over 1000 V.

Results and Discussion

The typical decay envelope for an uncontrolled beam (a baseline test) is shown in Fig. 8 in an oscilloscope photograph and a logarithmic plot. The upper trace in the oscilloscope photo is the feedback voltage and the lower trace the tip displacement. Even though the decay envelope of the displacement looks exponential, the logarithmic plot shows a slight change in the slope. (The logarithmic plot should be a straight line for exponential decay.) This indicates that the loss factor η changes with the amplitude. The loss factor at the large initial amplitudes (± 2 cm tip displacement) is slightly more than $\eta = 0.003$ decreasing to $\eta = 0.001$ for small amplitudes (± 0.5 mm tip displacement). This confirms the damping value obtained for small amplitude vibrations from the impact testing.

The results for the constant-gain controller for the two voltage limits are shown in Fig. 9 and 10. Since this is a linear controller, one expects the decay envelope to be exponential. However, as for the uncontrolled case, the slope of the logarithmic plots changes slightly. This is probably due to the amplitude dependence of the loss factor in the beam itself. For $V_{max} = 100$ V rms, the average loss factor is slightly less than $\eta = 0.006$ and slightly more than $\eta = 0.007$ for $V_{max} = 200$ V rms. This is an improvement over the baseline damping in the beam; but, as noted previously in the analysis, the feedback voltage decreases as the vibrations decay, indicating that better damping could be achieved at the smaller vibration amplitudes.

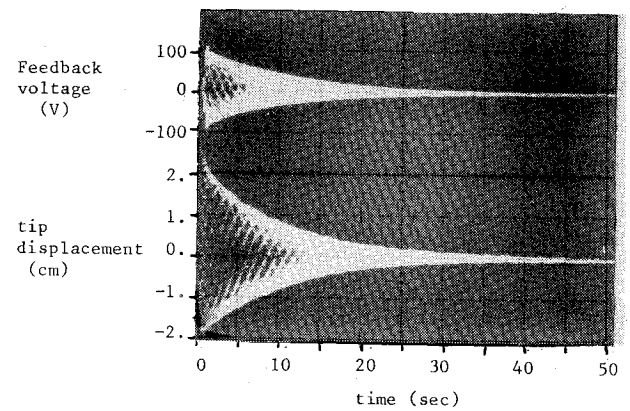

a) Feedback voltage and tip displacement for the uncontrolled beam.

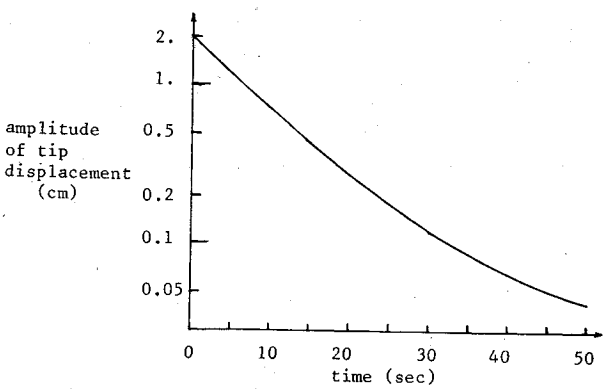

b) Logarithmic plot of tip displacement decay envelope.

Fig. 8 First-mode test results for the uncontrolled beam.

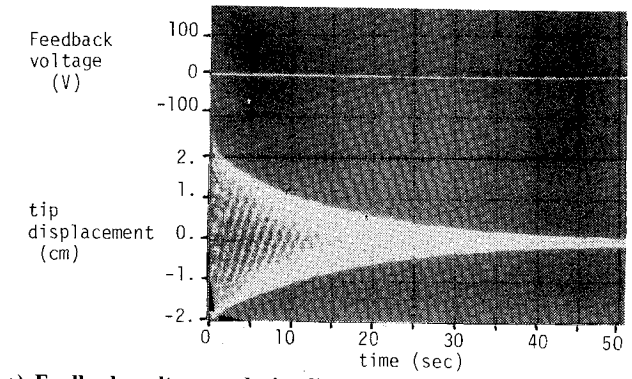

a) Feedback voltage and tip displacement for the constant-gain controller.

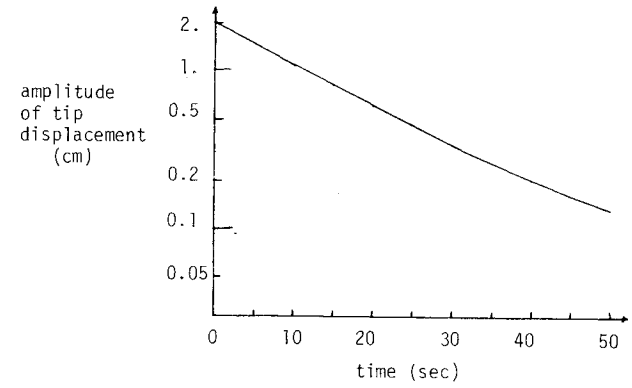

b) Logarithmic plot of tip displacement decay envelope.

Fig. 9 First-mode test results for the constant-gain controller, $V_{max} = 100$ V rms.

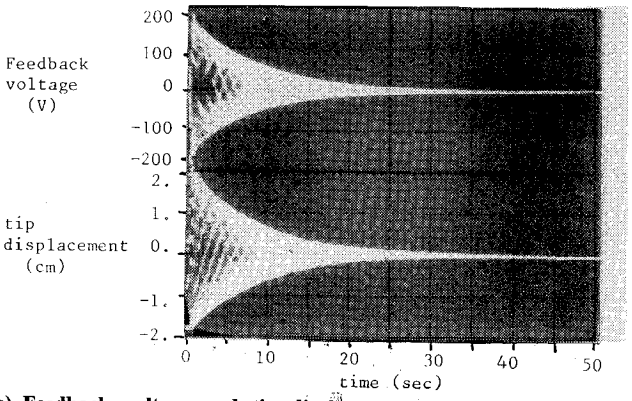

a) Feedback voltage and tip displacement for the constant-gain controller.

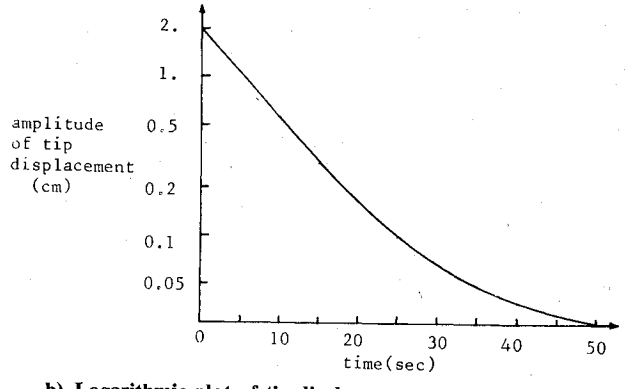

b) Logarithmic plot of tip displacement decay envelope.

Fig. 10 First-mode test results for the constant-gain controller, $V_{max} = 200$ V rms.

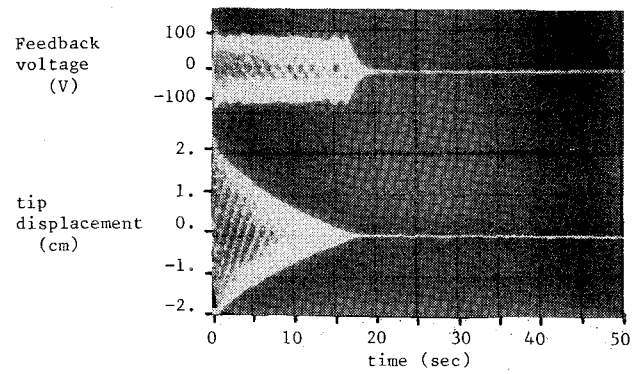

a) Feedback voltage and tip displacement for the constant-amplitude controller.

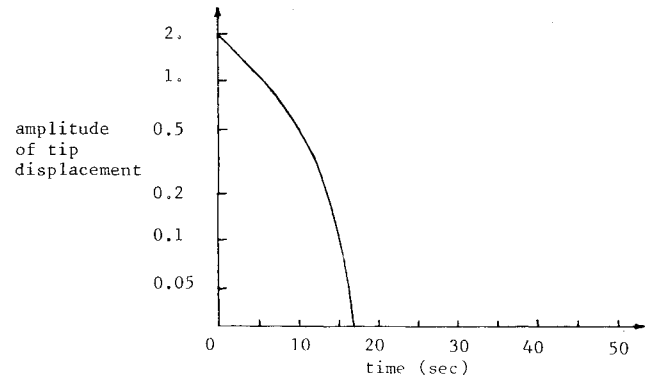

b) Logarithmic plot of tip displacement decay envelope.

Fig. 11 First-mode test results for the constant-amplitude controller, $V_{max} = 100$ V rms.

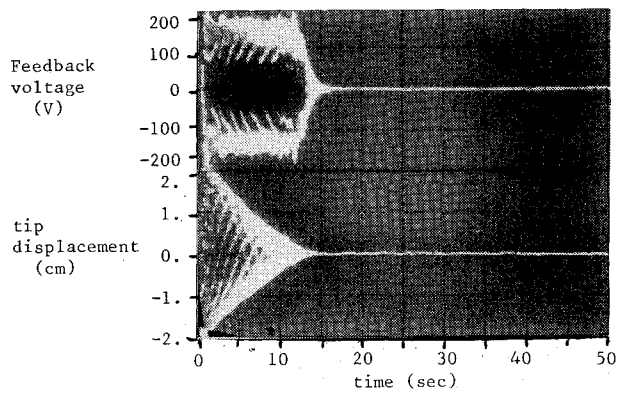

a) Feedback voltage and tip displacement for the constant-amplitude controller.

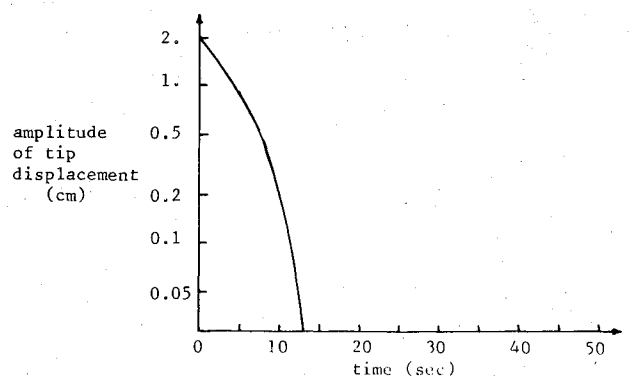

b) Logarithmic plot of tip displacement decay envelope.

Fig. 12 First-mode test results for the constant-amplitude controller, $V_{max} = 200$ V rms.

The results for the constant-amplitude controller, shown in Figs. 11 and 12, show a dramatic improvement over the constant-gain controller. With $V_{max} = 100$ V rms, the vibrations are totally damped in 18 s. For $V_{max} = 200$ V rms, the vibrations are damped in 15 s. The decay envelopes are nearly linear, which is expected for a nonlinear control of constant amplitude. The logarithmic plots show how dramatically the damping changes. For both voltage limits, the loss factor starts at the value achieved with the constant-gain controller and steadily increases to at least $\eta = 0.040$ for small amplitudes of vibration. This is at least a factor of 40 increase in the damping at small vibration levels. These results indicate that, while an active damper of this type may not work well for large amplitudes of vibration, it may provide a way to keep resonant vibration from building up since the highest level of damping is achieved for very small vibration levels. It may be possible to use this kind of active damper in conjunction with another more powerful actuator that will control the large-amplitude vibrations. Powerful actuators often have problems such as limit cycling or need a deadband at small vibration levels, providing a good complement to the active damper described here.

Conclusions

The control of distributed-parameter systems with discrete actuators and sensors and using lumped-parameter control theory may lead to performance tradeoffs. Using distributed-parameter control theory and distributed-parameter actuators one can avoid some of the tradeoffs, such as truncation of the model. An active distributed-parameter damper for a cantilever beam was designed and evaluated. The distributed-parameter active element was a piezoelectric polymer, poly (vinylidene fluoride). A control law was developed using Lyapunov's second method for distributed-parameter systems. Since no modes were truncated in the analysis, this control law will theoretically control all of the modes of vibration. This avoids any structural problems with uncontrolled modes.

Preliminary testing of the active damper was done using only the first mode of vibration of a small cantilever beam because the angular velocity of the tip of the beam was not available. The baseline loss factor for the first mode was 0.003 for large vibrations (±2 cm tip displacement), decreasing to 0.001 for small vibrations (±0.5 mm tip displacement). Three controllers were developed to test the damper on the first mode. Testing was performed using two of these controllers—the constant-gain and constant-amplitude controllers. The constant-gain controller was a linear controller and provided approximately double the baseline damping. The constant-amplitude controller was nonlinear and provided nonlinear damping—double the baseline loss factor for large vibrations inceasing by a factor of 40 to at least 0.040 for small vibrations. These results were achieved with a simple damper configuration, simple control algorithms, and moderate voltage levels compared to the breakdown voltage of the poly (vinylidene fluoride).

Acknowledgments

This work was supported by the Charles Stark Draper Laboratory as Independent Research and Development Project 181 during fiscal year 1984. The flexible satellite test structure was designed and built at the Draper Laboratory.

References

[1]Kelley, M.G., "Mechanical Design and Dynamic Scaling Considerations of a Flexible Spacecraft Test Model," B.S./M.S. Thesis, Massachusetts Institute of Technology, Cambridge, Mass., June 1983.

[2]Balas, M., "Feedback Control of Flexible Systems," *IEEE Transactions on Automatic Control*, Vol. AC-23, Aug. 1978, pp. 673-679.

[3]Ahmed, N.U. and Teo, K.L., *Optimal Control of Distributed Parameter Systems*, Elsevier North Holland, New York, 1981.

[4]Franke, D., "Distributed Parameter Systems," *Advances on Control Systems and Signal Processing,* Vol. 1, Friedrick Vieweg und Sohn, Wiesbaden, FRG, 1980.
[5]Komkov, V., *Optimal Control Theory for Damping of Vibrations of Simple Elastic Systems,* Springer-Verlag, Berlin, 1972.
[6]Lions, J.L., "Some Aspects of the Optimal Control of Distributed Parameter Systems," *Society for Industrial and Applied Mathematics,* 1972.
[7]Stavroulakis, P., ed., "Distributed System Theory: Part 1, Control," *Benchmark Papers in Electrical Engineering and Computer Science,* Vol. 26, Hutchinson Ross Publishing Co., Stroudsburg, Pa., 1983.
[8]Tzafestas, S.G., *Distributed Parameter Control Systems: Theory and Applications,* Pergamon Press, Elmsford, N.Y., 1982.
[9]Kalmann, R.E. and Bartram, J.E., "Control Systems Analysis and Design Via the 'Second' Method of Lyapunov," *Journal of Basic Engineering, Transactions of ASME,* 1960, pp. 371-400.
[10]Wang, P.K.C., "Stability Analysis of Elastic and Aeroelastic Systems via Lyapunov's Direct Method," *Journal of the Franklin Institute,* Vol. 281, No. 1, 1966, pp. 51-72.